Possible Air Separations with Superconducting Membranes

Ryan D. Gordon and E. L. Cussler
Dept. of Chemical Engineering and Materials Science, University of Minnesota, Minneapolis, MN 55455

Permeabilities of oxygen, nitrogen and helium across porous, superconducting membranes with 5-μm pores are consistent with those across nonsuperconducting membranes with well-defined pores of similar sizes. This is true both at ambient and superconducting temperatures. Transport can occur by Knudsen diffusion, Poiseuille flow, capillary condensation, and turbulent flow. There is no evidence of surface diffusion. Theoretical considerations of superconducting membranes are consistent with these results, indicating when superconductivity might play a role. However, past reports concerning air separation with superconducting membranes with these micrometer-sized pores are questionable.

Introduction

More oxygen and nitrogen are produced by the chemical industry than any other chemicals except sulfuric acid. More of each is made than ethylene or ammonia, those basic building blocks for petrochemicals and agrochemicals. Because of the commercial status of oxygen and nitrogen, their separation has major commercial value. Any new idea for separating these two merits careful attention.

At present, most air is separated by cryogenic distillation, a process which has considerably improved since its original patent in 1907. Such a cryogenic separation yields extremely pure gases, 99.999+% for nitrogen and 99.5–99.9% for oxygen. During the last ten years, pressure swing adsorption (Yang, 1987) and membrane separations (Koros and Fleming, 1993; Prasad et al., 1994) have gained a foothold. The growth of these noncryogenic techniques is due to the discovery of new applications and, in order to cut costs, the conversion of cryogenic customers to noncryogenic systems. Polymer membrane separations have special promise. In those commercially practiced, the smaller oxygen molecules (3.46 Å) pass through a nonporous, glassy polymer membrane, while the larger nitrogen molecules (3.64 Å) are retained (Robeson, 1991). The nitrogen-rich retentate, containing as much as 99% nitrogen, is then used, for example, to provide an inert atmosphere for storing fruit.

One exciting idea for separating oxygen from nitrogen is to use a porous, superconducting membrane. When pressurized air is forced through such a membrane, nitrogen is claimed to permeate and oxygen is retained (Reich and Cabasso, 1989). This is potentially an advantage, for the more valuable oxygen is kept at the higher feed pressure. Moreover, the flux across such a membrane is claimed to be more than one hundred times larger than the flux through existing commercial air separation membranes. Finally, the impurity argon presumably passes through the membrane with nitrogen, away from oxygen; the argon/oxygen separation is a significant fraction of the cost of cryogenic distillation. These major advantages are diluted by the low temperatures, around 100 K, required by current superconductors. This disadvantage might be minimized by using these membranes as a pretreatment for a conventional air distillation plant, where cold gases are already available.

There are plausible theoretical reasons to expect this separation to occur. Unlike nitrogen and argon, oxygen is paramagnetic. Hence, oxygen might be magnetically repelled from a perfectly diamagnetic superconductor. Such a Meissner effect is responsible for the popular laboratory demonstration of levitating a permanent magnet. Such an effect could alter oxygen transport in two ways. First, it could retard oxygen molecules as they approach the membrane, just as a Donnan potential can electrostatically retard ions diffusing towards a membrane. Secondly, the Meissner effect could cause the magnetic repulsion of oxygen molecules within the pores of the membrane, effectively making the pore radius smaller for oxygen, but not for nitrogen. The separation in this case would occur by molecular sieving.

Not surprisingly, the initial report of a superconducting membrane-based separation sparked efforts to duplicate the results. These new efforts were confusing. Some said the ef-

fect existed, but that the superconducting membranes were more permeable to oxygen (Sawai et al., 1995). Others said the effect did not exist (Louie, 1993). Still others reported dramatic differences in the surface adsorption, and possibly in surface diffusion, of oxygen and nitrogen on superconductors (Makarshin et al., 1997).

To illustrate these confusing efforts, we turn to an experiment of our own shown in Figure 1. In this experiment, cold pressurized air at 5 psig is forced across a porous, superconducting membrane of $(Bi,Pb)_2Sr_2Ca_2Cu_3O_x$ (BSCCO). The membrane had pores of around 5 μm in diameter. The data in Figure 1a show the effect of temperature on the permeate composition. At higher temperatures, where BSCCO is not superconducting, the permeate concentration is (0.21/0.79), or 0.27, the molar ratio of oxygen to nitrogen in air. The membrane has effected no separation. At temperatures well below 108 K, when the membrane is superconducting, the permeate concentration seems to drop, suggesting a nitrogen selective membrane. Later, the situation can change, and the permeate concentration can increase to as high as 0.45, suggesting an oxygen selective membrane.

The reasons for this erratic behavior can be seen more clearly from the data in Figure 1b. This figure shows both the permeate concentration and temperature plotted vs. time. When the membrane is warm, above the superconductor's critical temperature of 108 K, the permeate concentration is the expected 0.27. When the membrane is superconducting at lower temperatures, the permeate concentration oscillates wildly. The experiment, obviously not in steady state, may involve artifacts like capillary condensation of oxygen in the pores of the superconductor. However, it may also show influences of oxygen's paramagnetism.

This article explores and determines whether superconducting membranes can separate air, specifically whether the membrane's superconductivity alters the flux of oxygen. To do so, various effects possible as vapor flows through small pores at cryogenic temperatures are reviewed. Extensive permeation experiments both on superconducting membranes and on model membranes of known geometry are reported, as well as prospects for air separation based on porous membranes, including superconducting ones.

Theoretical Studies

In this work, the transport of oxygen and nitrogen in porous, superconducting membranes is compared with that in porous, nonsuperconducting membranes of well-defined geometry. This implies establishing two theoretical bases. First, the various mechanisms by which transport can occur in porous membranes must be reviewed. Secondly, it must be explored how these mechanisms can be altered by superconductivity.

Normal transport mechanisms

As we will show below, there are six different mechanisms by which transport can occur in porous membranes. The first three, binary diffusion, Knudsen diffusion, and Poiseuille flow, are expected. Two more, surface diffusion and capillary condensation, are often observed. The sixth, critical flow, is less common. Each of these mechanisms merits a brief review before discussing their behavior in superconductors.

In binary gas diffusion, molecules diffusing in pores collide much more frequently with other molecules than with the pore walls. This type of transport usually involves two different gases, and is most frequently studied at constant volume. The process is described by one diffusion coefficient D for each pair of gases; these are the diffusion coefficients tabulated in handbooks, and estimated with, for example, the Chapman-Enskog theory. Since gas-membrane interactions are relatively unimportant in this process, binary diffusion is not central to this research.

In Knudsen diffusion, molecules diffusing in pores collide much more frequently with the pore walls than with other diffusing molecules. Thus, gas-membrane interactions are central to the process. The Knudsen diffusion coefficient D_{Kn} can be estimated from the equation

$$D_{Kn} = \frac{d}{3}\left(\frac{2RT}{\tilde{M}}\right)^{1/2} \tag{1}$$

where d is the pore diameter and $\tilde{M}$ is the molecular weight of the diffusing species. Knudsen diffusion gives a different diffusion coefficient for each diffusing species, so a binary

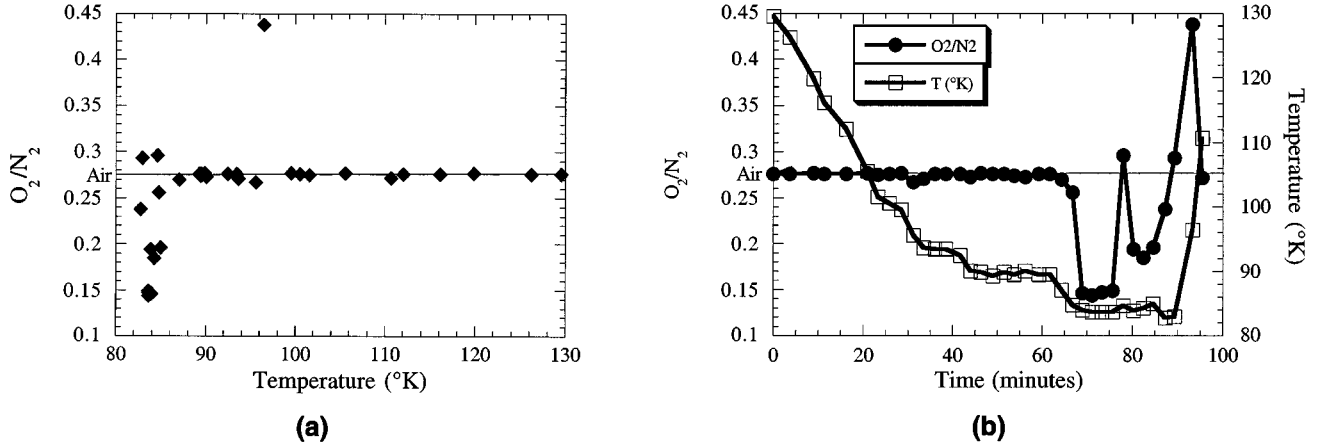

Figure 1. Air separation results for porous, superconducting membranes.

These results from our lab show the permeate composition after pumping air through a BSCCO membrane.

system has two different diffusion coefficients. This difference is sometimes suggested as a separation process using ceramic membranes, although the selectivity, based on the inverse square root of the molecular weights, is clearly modest. We also note that the Knudsen diffusion coefficient is independent of pressure. This mechanism will be important in our experiments.

The third mechanism, Poiseuille flow, relates the gas flux j_1 to its velocity v_1

$$j_1 = c_1 v_1 = \frac{p_1}{\mathrm{RT}}\left(\frac{d^2 \Delta p_1}{32 \eta \ell}\right) \tag{2}$$

where the concentration c_1 is proportional to the partial pressure p_1, the pore length is ℓ, and the transport coefficient is the viscosity η. For a single species, the appropriate partial pressure is the arithmetic average across the pore. As in binary diffusion, the gas molecules are colliding more frequently with each other than with the pore walls, so the chance of superconducting walls influencing the transport is small. We also note that the inferred ''diffusion coefficient'' from Poiseuille flow is a linear function of the partial pressure. This mechanism will also be important in our experiments.

Knudsen diffusion and Poiseuille flow often occur simultaneously. In this case, the total flux in one pore is commonly assumed to be the sum of the two mechanisms (Mason and Evans, 1969; Meixner and Dyer, 1998)

$$j_1 = \frac{D_{Kn} \Delta p_1}{\ell \,\mathrm{RT}} + \left(\frac{p_1 d^2}{32 \eta \ell}\right)\frac{\Delta p_1}{\mathrm{RT}} \tag{3}$$

Equation 3 is a typical result of the dusty-gas model (Mason and Malinauskas, 1983). Combining Eqs. 1 and 3 for a membrane with porosity ϵ and tortuosity τ gives the flux as

$$j_1 = \left[\frac{\frac{d}{3}\left(\frac{2\mathrm{RT}}{\tilde{\mathrm{M}}}\right)^{1/2} + \frac{p_1 d^2}{32\eta}}{\ell/(\epsilon/\tau)}\right]\frac{\Delta p_1}{\mathrm{RT}} = \frac{\mathrm{P}}{\ell}\frac{\Delta p_1}{\mathrm{RT}} \tag{4}$$

where P is the membrane's permeability, and the quantity P/ℓ is often called the permeance. We shall measure the permeability in most of the experiments described later in this article. We also note two limits that exist in Eq. 4. Transport in small pores or at low pressure is by Knudsen diffusion; transport in large pores or at high pressure is by Poiseuille flow.

We can rearrange Eq. 4 for the membrane's permeability to yield the equation

$$\frac{\mathrm{P}\tilde{\mathrm{M}}^{1/2}}{(\epsilon/\tau)d} = \left(\frac{\sqrt{2\mathrm{RT}}}{3}\right) + \left(\frac{1}{32\eta}\right)\frac{p_1 d}{\tilde{\mathrm{M}}^{1/2}} \tag{5}$$

We can use Eq. 5 to combine experiments with different membranes and different gases onto a single graph, plotting $\log[\mathrm{P}\tilde{\mathrm{M}}^{1/2}/d(\epsilon/\tau)]$ vs. $\log(p_1 d\tilde{\mathrm{M}}^{-1/2})$. To do so, we assume an average viscosity, which is reasonable since the viscosities of the light gases studied in our experiments are similar. If the data on such a graph are horizontal, we have Knudsen diffusion; if the data increase linearly, we have Poiseuille flow. We will often use this simple test.

Other transport mechanisms

Diffusion data can deviate from plots based on relations like Equation 5. These deviations are often attributed to two other transport mechanisms: surface diffusion and capillary condensation. Sometimes these mechanisms are cited uncritically, a convenient rationalization on which any unexpected behavior can be blamed. We want to review their behavior critically here, for we will try to apply them quantitatively.

Surface diffusion occurs when gas molecules adsorb onto the pore walls, and then diffuse (Yang, 1987). When the adsorption is physical, the adsorption is normally not selective, but the adsorbed species is highly mobile. When chemisorption occurs, the adsorption has a higher energy and a greater selectivity, but the adsorbed species is normally immobile, bound to specific sites. Because surface diffusion involves direct contact between the diffusing species and the solid, it is one of the mechanisms most likely to be affected by superconductivity.

Surface diffusion is normally measured as a deviation from the flux expected for a nonadsorbing gas, most often helium (Sircar and Rao, 1990). For example, when Knudsen diffusion is expected, we would expect the flux of nitrogen to be less than that of helium by the inverse square root of the ratio of molecular weights, as suggested by Eq. 1. If we observe a larger nitrogen flux, we could attribute the difference to surface diffusion. Alternatively, we expect that the observed permeabilities graphed according to Eq. 5 would be higher for any adsorbing species than for helium. We will use this second criterion to test for surface diffusion.

A second, less common mechanism for transport in these systems is capillary condensation. When a porous membrane is in contact with a vapor, the saturation vapor pressure in the pores p can differ from the saturation vapor pressure in the bulk p_o according to the Kelvin equation (Brunauer, 1945)

$$p = p_o e\left[\frac{\tilde{V}_L 4\gamma}{RT\,d}\cos\theta\right] \tag{6}$$

where $\tilde{V}_L$ is the molar volume of the liquid, δ is the surface tension of the liquid, d is the pore diameter, and θ is the contact angle between the liquid and the pore. If the pore is wet by the liquid, then θ is assumed to be zero. Capillary condensation is significant for small pores. For example, for nitrogen in 10 nm wetted pores, the saturation vapor pressure of nitrogen at 77 K is reduced from 760 mm Hg to 640 mm Hg, because the molar volume is 1.24 cm^3/g and the surface tension is 8.27 dynes/cm for liquid nitrogen at that temperature.

While the vapor pressure reduction in Eq. 6 is well verified at equilibrium (Gregg and Sing, 1982), its effect on transport is less well established (Uhlhorn et al., 1992). The most obvi-

ous possibility is that the resulting liquid moves by Poiseuille flow, according to Eq. 2, but with the concentration and viscosity of a liquid, not of a gas. Another possibility is that the liquid condensate flow is driven by surface forces, rather than by a pressure difference (Carman, 1956; Lee and Hwang, 1986). In either case, we would not expect this mechanism to be greatly influenced by superconductivity, except possibly through the surface tension.

A final less common transport mechanism possible in these membranes is critical flow. In this mechanism, the pores in the membrane are wide and very short. There is no Knudsen diffusion or viscous drag, because there is almost no pore wall: any molecule which enters the pore passes through. The flux in this case is independent of pressure and the permeability is independent of pressure (O'Neil and Chorlton, 1989). Note that in this mechanism, the Mach number of the gas in the pore equals one.

These mechanisms can be distinguished by plotting the data as suggested by Eq. 5. Surface diffusion is implicated when the results for nonadsorbing gases like helium agree with the permeabilities expected from this plot, but the permeabilities of the adsorbing species are higher. Capillary condensation may cause deviations from Eq. 5 whenever Eq. 6 suggests that capillary condensation is feasible. Critical flow will occur at higher pressures, where the pore diameter is larger than both the mean free path of the gas and the thickness of the membrane.

Superconducting mechanisms

On the basis of this discussion, we now explore how superconducting membranes might alter the transport of a paramagnetic gas like oxygen. These effects could occur either outside the membrane or inside the pores of the membrane. To understand these effects, we briefly describe the physics of superconductivity.

A superconductor exhibits a remarkable combination of electric and magnetic properties (Rose-Innes and Rhoderick, 1969). Below its critical transition temperature, a superconductor enters a superconducting state in which it not only loses its electrical resistance, but is also perfectly diamagnetic. A perfectly diamagnetic material repels a magnetic field away from its surface, preventing the field from completely penetrating into the material; the field will penetrate to a ''penetration depth'' of about 100 nm into the superconductor (Orlando and Delin, 1991). A popular demonstration of this phenomenon, called the Meissner effect, is to levitate a permanent magnet above a superconductor. An external magnetic field greater than a critical field strength will penetrate into the superconductor and quench its superconductivity. Under these conditions, the superconductor is no longer perfectly diamagnetic.

A superconductor will alter the chemical potential μ_1 of an oxygen molecule as follows

$$\mu_1 = \mu_1^0 + \frac{5}{2}\mathrm{kT} + \mathrm{kT}\ln c_1 + 2\mu\mathrm{B} \tag{7}$$

The first three terms on the righthand side of this expression are familiar: μ_1^0 is a reference value; (5/2) kT is the thermal energy of the oxygen; and the logarithmic term is the entropic contribution. The fourth term, which is less familiar, is the magnetic energy: it is the product of oxygen's magnetic moment μ and the magnetic flux density B. This term arises because of the magnetic repulsion between a paramagnetic oxygen molecule and its reduced magnetic image within the superconductor (Hellman et al., 1988). For a magnetized sphere, the flux density is given by (Jackson, 1962)

$$\mathrm{B} = \frac{2\mu_0\mu}{r^3} \tag{8}$$

where μ_0 is the magnetic permeability and r is the distance between the molecule and its induced magnetic image within the superconductor. In more practical terms, r is twice the distance between the oxygen molecule and the superconductor's boundary.

While calculating the exact effect of the magnetically altered chemical potential is difficult, we can qualitatively understand the effects involved by considering three special cases. These are alterations within the pore, at the mouth of the pore, and approaching the superconducting membrane. Within the pore, we are concerned only with single molecules, so the entropic term is not involved. In this case, Eqs. 7 and 8 can be combined to give

$$\mu_1 = \mu_1^0 + \frac{5}{2}\mathrm{kT}\left[1 + \left(\frac{\delta}{r}\right)^3\right] \tag{9}$$

where the characteristic distance δ equals

$$\delta = \left(\frac{8\mu_0\mu^2}{5\mathrm{kT}}\right)^{1/3} \tag{10}$$

Superconductivity will strongly affect oxygen transport when δ is the same size as the pore radius. This effect, which could be regarded as sieving, is that discussed in an earlier study (Reich and Cabasso, 1989).

Superconductivity could also affect oxygen transport near the mouth of the pore. There, we expect an equilibrium

$$\mu_1\,(\text{inside}) = \mu_1\,(\text{outside}) \tag{11}$$

Because the superconductivity would have little effect outside, we can combine Eqs. 7, 8, and 11 to find

$$c_1\,(\text{inside}) = \mathrm{K}c_1\,(\text{outside}) \tag{12}$$

In Eq. 12, the partition coefficient K is given by

$$\mathrm{K} = e^{-12(\delta/d)^3} \tag{13}$$

where d is the pore diameter and δ is again given by Eq. 10. This possibility does not seem to have been discussed previously. Note that for larger pores (above the Knudsen limit), the total pressure will be continuous across the pore mouth. Thus, the reduced oxygen concentration suggested by Eq. 12 will effect an increased nitrogen concentration and enhanced membrane selectivity.

Finally, superconductivity could repel oxygen molecules as they approached the membrane. This idea, like the levitation of a permanent magnet but on a molecular scale, has been explored as a possible cause of these effects (Sawai et al., 1995). Its careful development begins with the equation for the total oxygen flux n_1 (Cussler, 1997)

$$n_1 = j_1 + c_1 v^o \tag{14}$$

where j_1 is the diffusion flux and v^o is the convective velocity sweeping oxygen towards the surface. The diffusion flux is in turn given by

$$-j_1 = \frac{Dc_1}{kT}\frac{\partial \mu_1}{\partial z} \tag{15}$$

where z is the distance normal to the membrane. Combining Eqs. 7, 8, 10, 14 and 15 we find

$$n_1 = -\frac{D\,dc_1}{dz} + c_1\left(v^o + \frac{45D}{4}\left(\frac{\delta^3}{z^4}\right)\right) \tag{16}$$

The detailed solution will depend on the boundary conditions chosen; the film and penetration theories of mass transfer are two obvious choices. For our purposes, the key point is the appearance of the characteristic distance δ, the common parameter in each of the three models. We will return to these theoretical results after we describe the experiments.

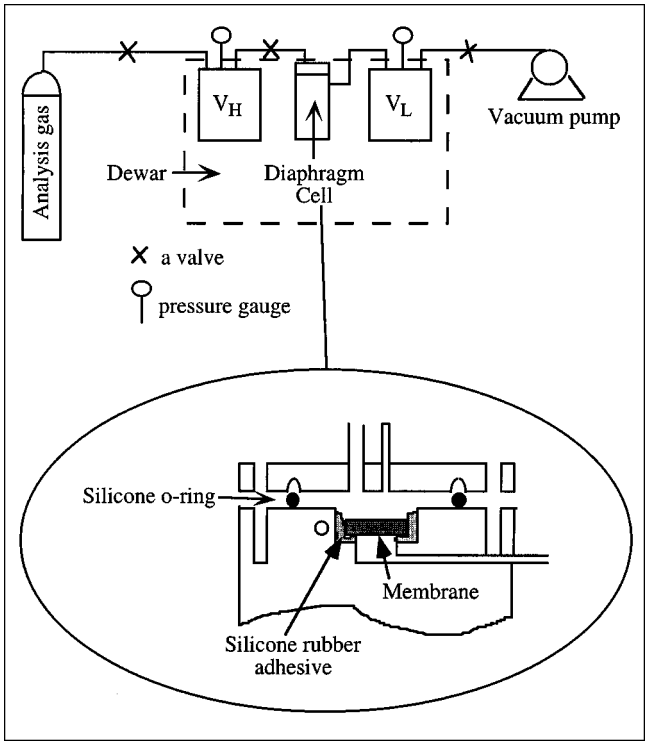

Figure 2. Diaphragm cell used for the batch diffusion experiments.

Experimental Studies

We determined the transport mechanism of oxygen and nitrogen by measuring the permeabilities of these gases across both superconducting and nonsuperconducting membranes. We used a diaphragm cell to measure gas permeabilities. We chose the diaphragm cell for its analytical and experimental simplicity. Because the cell operates isothermally with a constant amount of gas in the system, experimental artifacts are minimized. No moving parts and no forced convection of gas exist to complicate either the experiment or the analysis.

We used this diaphragm cell to measure single and mixed gas permeabilities through porous membranes. The cell, shown in Figure 2, consisted of two sections. The bottom piece contained a cavity into which the membrane was placed. This cavity measured 1.91 cm wide and 0.79 cm deep. Beneath this cavity was a smaller cavity, measuring 0.95 cm wide and 0.48 cm deep, that served as part of the low-pressure volume of the cell. The top piece of the cell was connected to the bottom with four hex screws. A silicone O-ring was placed between the two pieces to prevent gas leaks. The entire cell was made of brass, which is a diamagnetic metal.

The high- and low-pressure sides of the diaphragm cell were attached by stainless steel tubing to larger compartments. A two-way valve separated the high-pressure compartment from the diaphragm cell during gas loading. Both high- and low-pressure compartments were attached to a Duo-Seal vacuum pump (W. M. Welch Manufacturing Company) and a cylinder of the analysis gas. Two three-way valves isolated the diaphragm cell system from the environment. Two digital pressure gauges (Cole Parmer) were used to measure the pressures on the high- and low-pressure compartments. A type T thermocouple coated with Teflon (Cole Parmer) was used to measure the temperature. The thermocouple was glued inside a hole that extended through the metal of the diaphragm cell to within a millimeter of the membrane, but without penetrating the interior volume.

Inside the cell, the supported membrane served as the barrier between the upper and lower cavities of the cell. We mounted the membranes in the cell with silicone adhesive rather than a gasket to avoid cracking the ceramic membranes. Because some membranes were thin ($< 100\ \mu$m), we glued these membranes between two porous brass supports. Since we could control the area of the membrane exposed to gas by varying the area of the support, the supports acted as masks, allowing us to change the time needed for the experiments.

We measured isothermal gas permeabilities at 293 K and 77 K. The former was easily performed in air under ambient conditions. For the latter, the diaphragm cell was placed into a large, foam-insulated dewar that contained liquid nitrogen. The valves and pressure gauges were not immersed into the liquid nitrogen, because they fail at 77 K. Thermal transpiration in the stainless steel tubing between the warm gauges and warm valves and the cold diaphragm cell did not alter the pressure measurements because the inside diameter of the tubing was too large for significant thermal transpiration (Ross and Olivier, 1964).

We studied the permeability of three different gases through each membrane. Ultra-pure carrier grade (99.999%; Air Products) nitrogen and ultra-pure carrier grade (99.996%; Air Products) oxygen were the focus of the research. We also

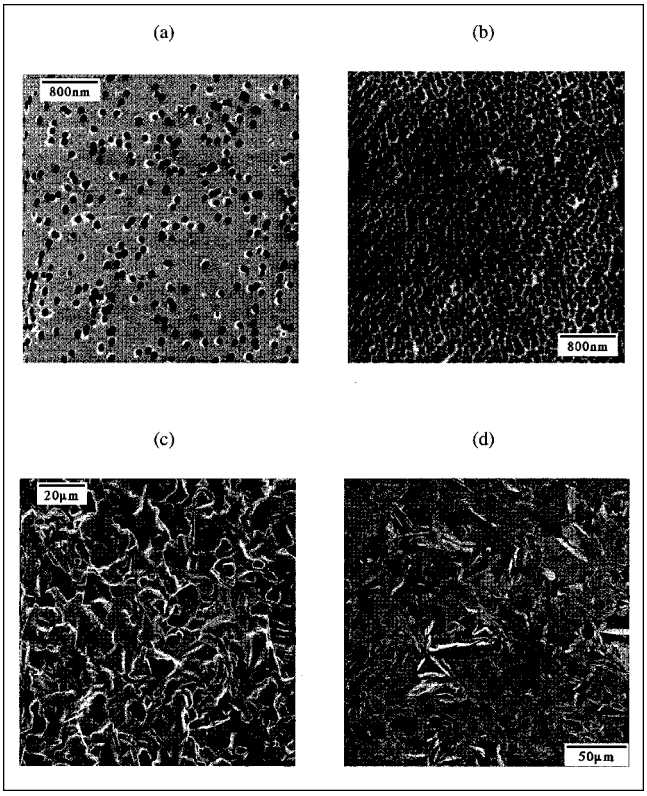

Figure 3. Scanning electron micrographs of the four types of membranes.

(a) 0.1 μm PCTE; (b) 0.1 μm Anodisc; (c) YBCO pellet; (d) BSCCO pellet.

measured the permeability of research grade (99.999%; Air Products) helium. Since helium's critical temperature is 5.1 K, its transport is only by Poiseuille flow and Knudsen diffusion. The transport of nitrogen and oxygen may be dramatically different due to magnetic repulsion, surface diffusion, or capillary condensation. If the latter mechanisms contribute significantly, then they will be obvious when the data are compared to those for helium.

The three types of membranes used in this work are dramatically different, as shown by the micrographs in Figure 3. The track-etched polycarbonate (PCTE) membranes (Poretics), shown in Figure 3a, are formed by etching radiation-damaged polycarbonate to produce monodisperse, near-cylindrical pores with minimal tortuosity. Though these membranes are not superconducting, their well defined pore geometry makes them excellent models. The second type is the Anodisc membrane (Whatman) formed electrochemically of alumina (cf. Figure 3b). These membranes are also not superconducting, but their monodisperse pores make them good models of higher porosity than the PCTE membranes. The manufacturers' specifications for the pore diameters, porosities, and thicknesses of the PCTE and Anodisc membranes that we analyzed are shown in Table 1. Both types of membranes were 13 mm in diameter, small enough to fit into the upper cavity of the diaphragm cell. Table 1 also gives the BET surface areas of these membranes, measured with a Micromeritics ASAP 2000 adsorption apparatus.

Table 1. Pore Geometry Specifications and Data for the Membranes Analyzed by the Batch Diffusion Experiment*

Membrane	Pore Dia. (μm)	Thickness (μm)	Porosity	Surface Area (m^2/g)
PCTE	0.01	6	0.00047	0.96*
PCTE	0.1	6	0.031	2.76*
PCTE	1	11	0.157	1.33*
PCTE	10	10	0.079	0.20*
Anodisc	0.02	60	0.25	3.12*
Anodisc	0.1	60	0.4	5.59*
YBCO	6.1*	300*	0.080*	0.059*
BSCCO	5.2*	400*	0.093*	0.10*

*Unless specified by *, all values were supplied by the membrane manufacturer. Values specified by * were measured by us.

The third type of membrane that we analyzed is the focus of our work, the porous ceramic superconductor. We analyzed two different high-temperature superconducting membranes, $YBa_2Cu_3O_{7-x}$ (YBCO) and the $(Bi,Pb)_2Sr_2Ca_2Cu_3O_x$ (BSCCO) (Colorado Superconductor, Inc.), shown in Figures 3c and 3d, respectively. Both membranes were formed by a solid-state reaction, pressing precursor powder into a pellet at high pressure and then sintering and annealing the pellet to obtain the desired oxygen stoichiometry. This process creates a much more heterogeneous pore size than that found in the model membranes. Besides polydispersity, these membranes also have large average pore diameters, on the order of 5 μm, and a tortuous pore structure. Obtaining the more desirable smaller, uniform pores will require a different method of membrane manufacture. The physical specifications of each superconducting membrane are also provided in Table 1. The diameters of these membranes were 15 mm, small enough to fit into the diaphragm cell. Again, BET surface areas were measured with equilibrium nitrogen adsorption. The average pore diameters and the ratio of the porosity to the tortuosity were calculated from permeability measurements with the diaphragm cell (Meixner and Dyer, 1998).

Because we are interested in determining if superconductivity influences the transport of a paramagnetic gas through a superconducting membrane, we need to address two other important properties of these materials. These are the critical temperature (T_c) and the magnetic moment. Both are measures of the quality of the superconductor. The former is a measure of when the material becomes superconducting and the latter is an indication of how much of the material is actually superconducting.

We measured the T_c of representative porous pellets of YBCO and BSCCO with a four-point probe (Bourdillon and Bourdillon, 1994). Although these were not the membranes that we used for the permeability measurements, they were manufactured identically. The T_c was 94 K for YBCO, as expected, and 92 K for BSCCO. The low T_c for BSCCO suggests that the stoichiometry may be closer to that of $Bi_2Sr_2Ca_1Cu_2O_x$, another superconductor with a T_c of 85 K. The transitions for both materials are broad, indicating that the pellets are polycrystalline. We did not quantitatively determine the T_c of each superconducting membrane before and after the permeability measurements. Rather, we crudely measured superconductivity by floating a small neodymium-iron-boride magnet above the membrane at 77 K to observe

the Meissner effect. For all YBCO and BSCCO membranes used in the diaphragm cell experiments, the magnet floated both before and after the permeability experiments were performed. This assured us that the membrane's superconductivity was not dramatically altered during the experiment.

We did not measure the magnetic moment for any of the superconducting membranes analyzed with the diaphragm cell. Instead, we relied on magnetometer measurements (Bourdillon and Bourdillon, 1994) for YBCO and BSCCO superconducting powders (Praxair Speciality Ceramics). Because both the membranes and the powders are polycrystalline, they should possess similar superconducting properties. Based on this supposition, each membrane is about 70% superconducting at 77 K.

The procedure to determine the permeability of all these membranes consisted of two steps. First, the high-pressure compartment was charged with gas; a vacuum existed inside the low-pressure compartment. The temperature of the gas was allowed to equilibrate to the desired experimental temperature. Then, the valve between the high-pressure compartment and the diaphragm cell was opened. Next, the pressures of both the high- and low-pressure sides of the membrane were measured as time proceeded. The experiment ended when the pressure drop across the membrane was less than 10% of its original value. The experimental time for a given membrane was controlled by varying the volume of the diaphragm cell and the area of the membrane exposed to gas.

Data from these experiments are analyzed with the normal diaphragm cell equation (Cussler, 1997)

$$\ell n\left[\frac{p_H(0)+p_L(0)}{p_H(t)-p_L(t)}\right]=\beta Pt \tag{17}$$

where p_H and p_L are the pressures on the high-pressure and low-pressure compartments, respectively, t is the time, P is the membrane's permeability, and β is a geometric factor. This factor is given by

$$\beta=\frac{A}{\ell}\left(\frac{1}{V_H}+\frac{1}{V_L}\right) \tag{18}$$

where A is the membrane's area, ℓ is its thickness, and V_H and V_L are the volumes of the high- and low-pressure compartments. All these variables were known before performing each experiment. In the batch experiments, both p_H and p_L actually changed with time, and represented the only dependent variables.

In addition to the batch experiments, we also performed flow experiments which were continuously fed with air on the high-pressure side of the membrane. The flow cell is the same nonferromagnetic brass cell that we used for the batch diffusion experiments. The only difference in the cell is that the feed in the flow experiment is swept across the membrane, so the high-pressure side has a gas outlet vented to the atmosphere. Again, we used a silicone O-ring and hex screws to seal the cell. We made flow experiments with superconducting and nonsuperconducting membranes. These membranes, the same as those in Table 1, were glued into the cell with silicone adhesive. Porous brass masks were also used to reinforce the thin, nonsuperconducting membranes. The flow system is shown in Figure 4. Ultra-pure carrier grade (99.999%; Air Products) air was used as a feed; its pressure was regulated at the air cylinder. The permeate stream flowed first through an 8-port switching valve (Valco Instruments Co., Inc.), where it was mixed with helium, and then to a gas chromatograph (Hewlett-Packard 5890) fitted with a column containing molecular sieve 5A support (Alltech) and a thermal conductivity detector. The chromatograph was calibrated with three oxygen/nitrogen gas mixtures prior to each experiment: 1/99, 10/90, and 21/79 (in percent). The flow rate of the permeate, measured beyond the switching valve with a bubble meter, was typically 2 mL/s for an upstream pressure of 5 psig (34 kPa). Once the desired temperature was reached, the experiment continued for a minimum of one hour, with the permeate stream composition being measured every two minutes. The upstream and downstream pressures, the temperature, and the permeate flow rate were also monitored continuously.

Controlling the operating pressure and temperature in this flow experiment is crucial. The temperature must be maintained between the critical temperature of the superconductor and the dew point of air at 5 psig. The critical temperature is above 90 K for YBCO and BSCCO, and the dew point of air at 5 psig is 84 K (Dodge and Dunbar, 1927). Above this range, the membrane is not superconducting: the permeate composition will be that of air. Below this range, the gas condenses, forming a two-phase mixture: the permeate composition should reflect the vapor-liquid equilibrium.

Results

The results of this work are most easily described as two categories: membrane permeabilities and anomalies. Each is described in the following paragraphs.

Membrane permeabilities

The results of a typical batch diffusion experiment are shown in Figure 5a. The specific membrane used was 0.33 cm^2 of a YBCO pellet, operated at 293 K and an initial pres-

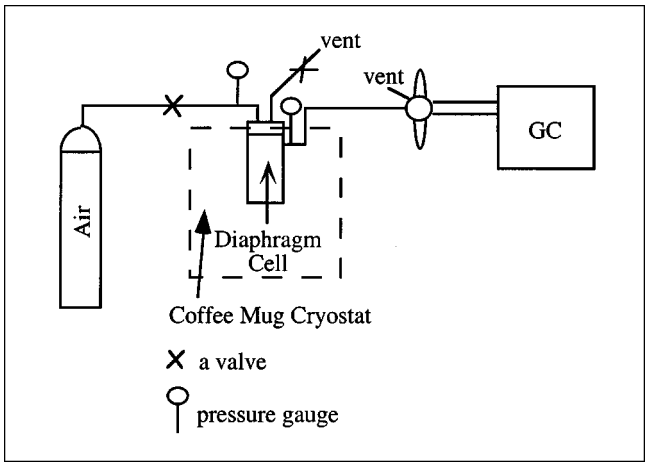

Figure 4. System used for the cryogenic flow experiments.

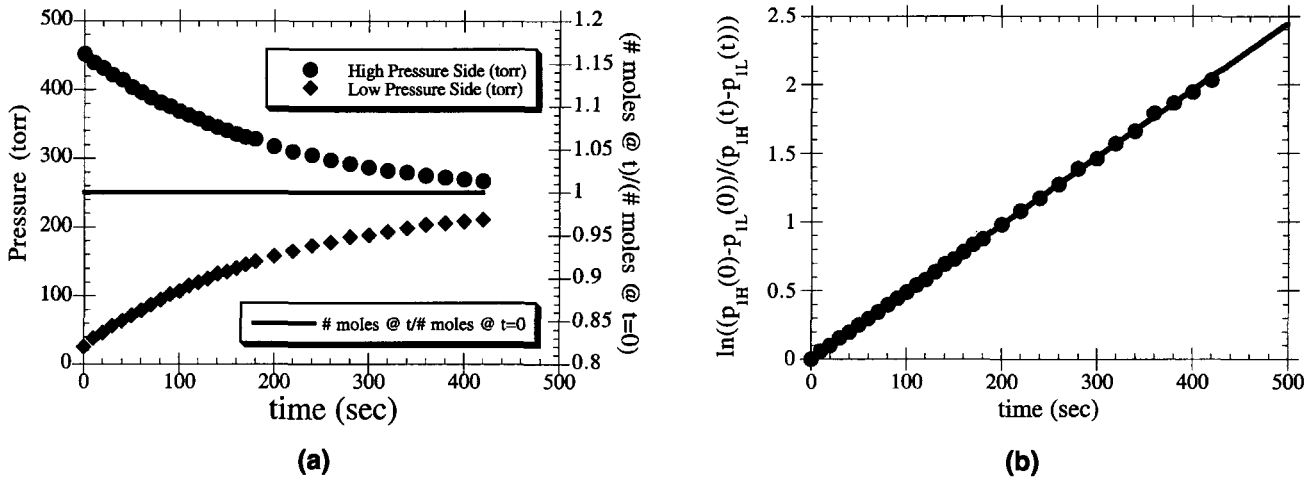

Figure 5. Typical results for oxygen and a YBCO membrane at 293 K.

(a) Raw data; (b) raw data plotted according to Eq. 17.

sure of 450 torr in the high-pressure compartment. The plot shows the expected transient behavior, a decay in absolute pressure of oxygen in the high-pressure volume and a rise in absolute pressure in the low-pressure volume. The total oxygen pressure in the system, shown as the solid line between the data points, is constant, evidence of a leak-free system. The data are replotted in Figure 5b according to Eq. 17. The slope of these data is a measure of the membrane's permeability.

We made two groups of membrane permeability experiments for one gas at a time. In the first group, shown in Figure 6, the temperature was ambient, 293 K. The data are for four different pore sizes of PCTE membranes, two different pore sizes of Anodisc membranes, and one pore size of each of two different superconductors. Pore geometry specifications for each membrane are provided in Table 1. The membrane permeabilities presented in Figure 6 were measured for three different gases. Helium was chosen because it is nonadsorbing; oxygen and nitrogen are the focus of this research.

The data in Figure 6 are plotted according to Eq. 5. The abscissa, the independent variable, includes the pore diame-

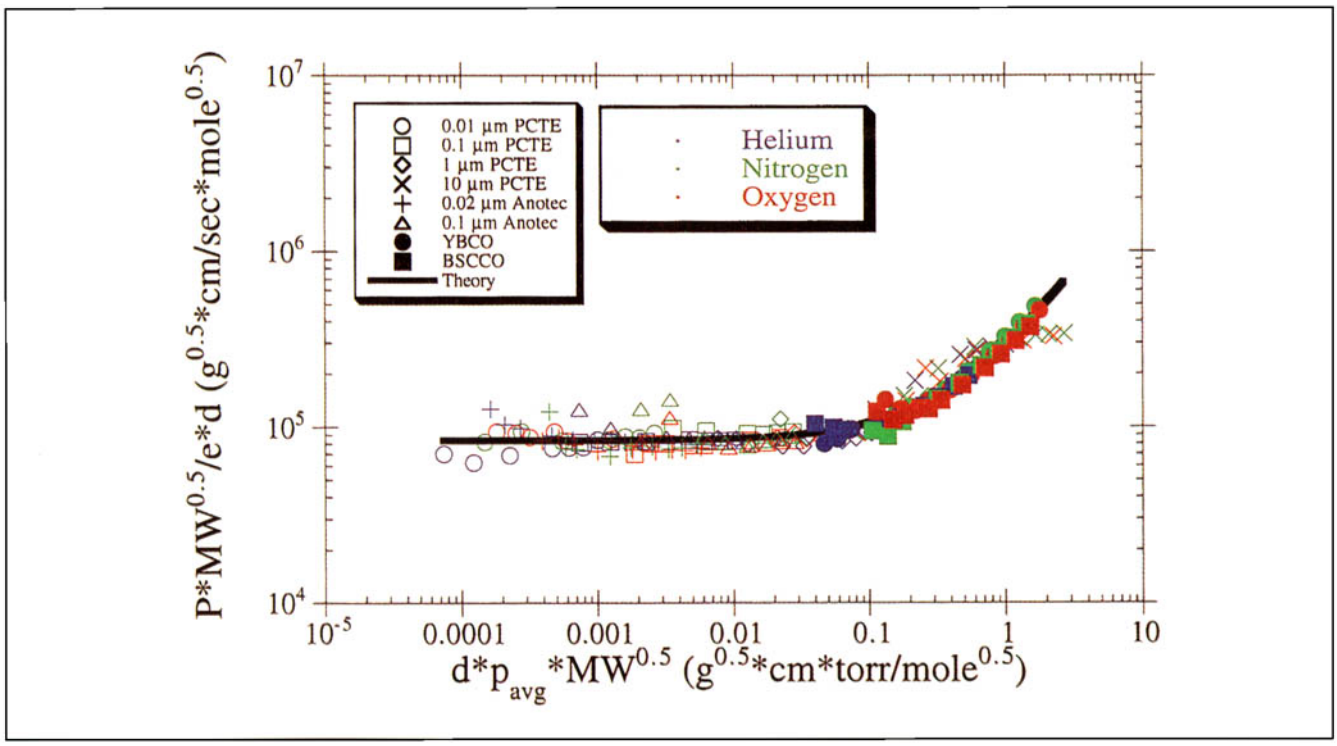

Figure 6. Diaphragm cell experiments at 293 K.

The data are plotted according to Eq. 5.

ter d, the arithmetic average pressure p between the two compartments, and the square root of the molecular weight of the diffusing gas $\tilde{M}^{1/2}$. The ordinate, which is the dependent variable, includes the membrane permeability, P, the pore diameter, the square root of the molecular weight of the gas, and the ratio of the membrane's porosity to its tortuosity ϵ/τ. The data on the abscissa vary by more than 10^4; those on the ordinate vary by a factor of 10.

Since the data in Figure 6 agree with the theory represented by Eq. 5, they imply that the only transport mechanisms operating at 293 K are Knudsen diffusion and Poiseuille flow. At low pressure and small pore diameter, the values of $P\tilde{M}^{1/2}/d(\epsilon/\tau)$ are constant, as predicted for Knudsen diffusion. For higher pressures and larger pores, the values of this combined parameter vary linearly with $dp\tilde{M}^{1/2}$ just as expected. No significant surface diffusion is observed at 293 K. If it occurred, then the permeabilities of adsorbing species like oxygen and nitrogen would fall above both the theoretical line and the permeabilities of the nonadsorbing helium. In Figure 6, these data overlap.

Significantly, the data for the superconducting membranes are consistent with those of the nonsuperconducting, model membranes. This is not surprising, for no superconductivity is expected in these membranes at 293 K. Nonetheless, this observation is important, because it suggests that we have characterized the flow of gases through these membranes effectively. Effects of chemical instability are not evident. Our use of an average pore diameter is reasonable even though the superconducting membranes have polydisperse pores.

The second group of membrane permeability experiments were similar but at 77 K, where superconductivity does occur in the YBCO and BSCCO membranes. We want to see if the oxygen permeability is suddenly altered by the magnetic repulsion from the superconducting membrane, as suggested in previous work. The results at 77 K are plotted in Figure 7 in the same way as the results at 293 K are plotted in Figure 6. The scatter in these cryogenic results is larger, a consequence of the greater experimental difficulties of working at low temperatures. There are significant deviations from the single correlating curve under some conditions, and these will be discussed later. Still, the overall conclusion drawn from Figure 7 is that most data are well correlated with this plot.

As with the data collected at 293 K, most of the data in Figure 7 suggest that helium, nitrogen, and oxygen pass through the membranes by either Knudsen diffusion and Poiseuille flow. In particular, the results of the superconducting YBCO and BSCCO membranes shown in Figure 7 are indistinguishable from the results with the nonsuperconducting, model membranes. The results for oxygen are consistent with those for nitrogen and for helium. Each gas flows by Poiseuille flow through the superconductors both at 293 K, where these membranes are not superconducting, and at 77 K, where these membranes are superconducting. Superconductivity has no measurable effect on the permeability of oxygen in the membranes used in these experiments.

This conclusion must be tempered by the fact that transport in the particular superconducting membranes which we used was always by Poiseuille flow. From the theoretical arguments given earlier, we expect that the effects of superconductivity will be most likely when the diffusing species frequently interact with the pore walls. In Poiseuille flow, such interactions are infrequent. We tried to increase the interactions between the diffusing gas and the superconducting surface by performing experiments at much lower pressures,

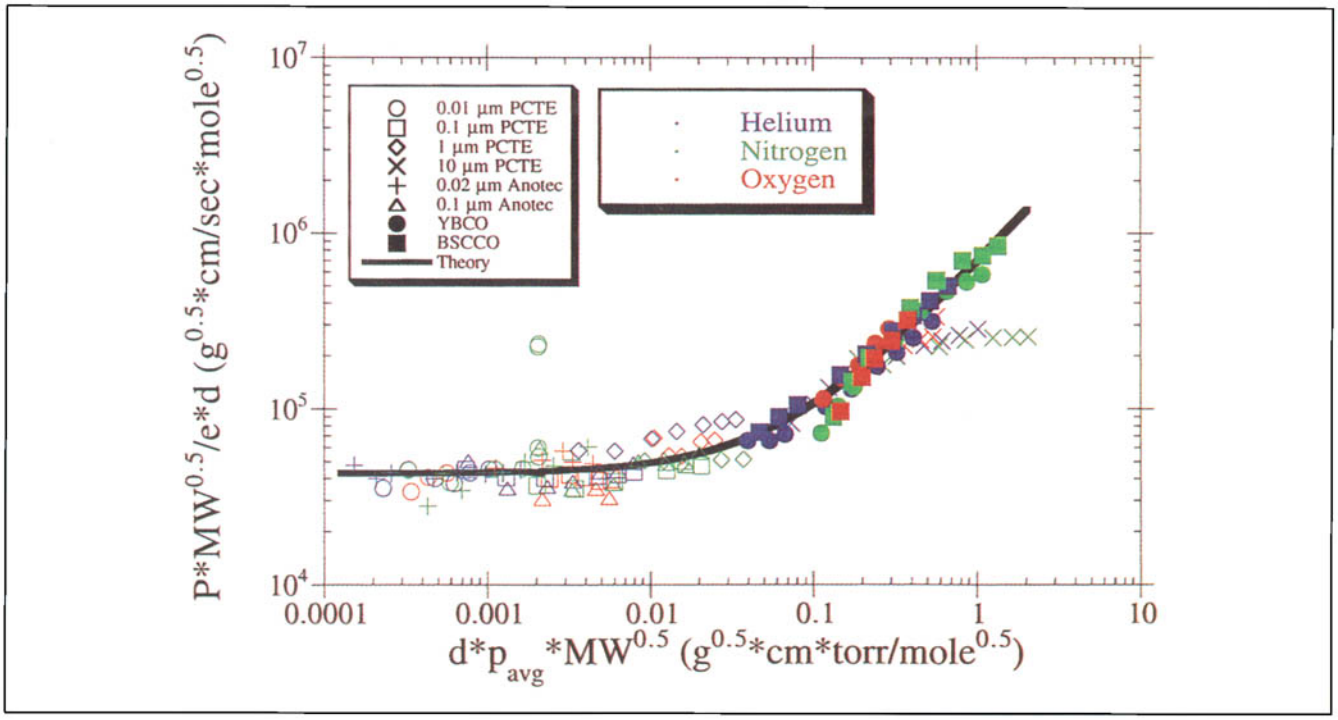

Figure 7. Diaphragm cell experiments at 77 K.

These data are also plotted according to Eq. 5.

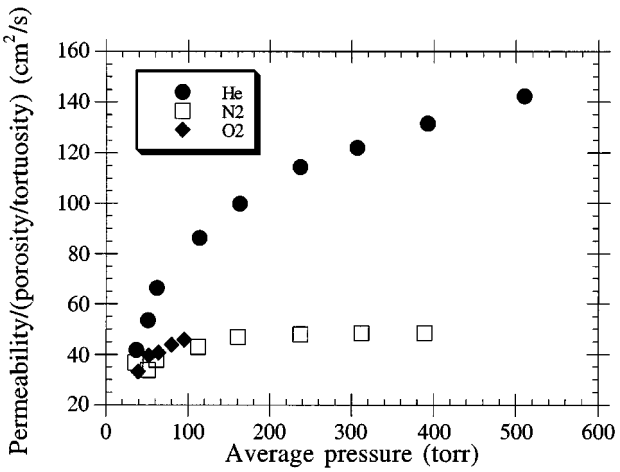

Figure 8. Permeability results for the 10-μm PCTE membrane at 77 K on non-normalized axes.

where transport would be by Knudsen diffusion. However, the pressures required, below 10 torr, were beyond the reach of our apparatus.

Other transport mechanisms

The results in Figure 7 do show transport mechanisms other than Knudsen diffusion and Poiseuille flow. While these mechanisms do not involve superconductors, they are interesting. There is still no evidence of surface diffusion: like Figure 6, the oxygen and nitrogen fluxes in Figure 7 are consistent with the helium flux. The low specific surface areas of the model membranes, given in Table 1, suggest that surface diffusion will not be an important source of flux through these membranes.

However, the data in Figure 7 do provide evidence of both turbulent flow and capillary condensation. The evidence for turbulent flow is best seen in Figure 8, which replots the data for the 10 μm PCTE membranes on non-normalized axes. These data, at 77 K, include measurements with oxygen, nitrogen, and helium, so the effect is not due to a particular gas. The effect in Figure 8 was obtained with several membranes, and so is not due to one anomalous membrane. The membranes are track-etched, so that polydispersity of the pores is small. The membranes are polycarbonate, and the other polycarbonate membranes with smaller pores are well-behaved, so no chemical artifacts exist.

The data in Figure 8 show that for these particular membranes at low pressures, the permeability increases with the average pressure, but with $p^{1/2}$, not $p^{1.0}$ as expected for Poiseuille flow. The data at 293 K give a similar result. The data in Figure 8 show that at higher pressures the permeability becomes nearly constant. This cannot be due to Knudsen diffusion or molecular effusion (Mason and Kronstadt, 1967), for the mean free path of each gas under these conditions is less than 0.1 μm, much less than the pore diameter.

Thus, these flows must be due to a different mechanism than those discussed previously. The length-to-diameter ratio in these pores is about one, according to the manufacturer's specifications in Table 1. Viscous flow is unlikely in such a short, wide pore, since little pore wall exists to create a viscous drag. A critical flow might exist in such a pore, but the data do not support this mechanism. The flow is subsonic, with the Mach number never exceeding 0.5. Therefore, we believe that the results in Figure 8 reflect turbulence created by entrance effects of the gas crossing the orifice-like pore. In this case, inertial forces will dominate viscous forces. Lighter gases, like helium, will flow faster through the pore than heavier gases, like oxygen and nitrogen. The data in Figure 8 reflect this phenomenon.

There is also evidence for capillary condensation at 77°C in the membranes with smaller pores. The particular data of interest are for nitrogen in the 0.01 μm PCTE membrane whose coordinates in Figure 7 are (0.002, 200,000). These data were obtained for several membranes, so were not the result of one quirky membrane. In this experiment, the initial pressure of nitrogen on the high-pressure side of the membrane was 750 torr, only slightly less than the equilibrium vapor pressure of 760 torr. The initial pressure on the low-pressure side of the membrane was zero. We note these pressures, because if the pores are wet with liquid nitrogen, then according to the Kelvin equation, the saturation vapor pressure of liquid inside the 0.01 μm pores will be 640 torr.

The details of this diffusion experiment are shown in Figure 9. As in Figure 5b, the function of pressure given in Eq. 17 is plotted against time. Two linear regions exist, instead of the one region in Figure 5b. The break between these two regions occurs when the high pressure in the cell has decreased to 690 torr, close to the expected equilibrium vapor pressure of 640 torr. The difference may be due to incomplete wetting or to somewhat larger pores, as the saturation vapor pressure of nitrogen at 77 K in a 0.02 μm pore is 690 torr.

We believe that at the lower pressures occurring at large times, transport is by Knudsen diffusion. In this region, characterized by the line with smaller slope in Figure 9, the pores contain only nitrogen vapor and no liquid nitrogen. Indeed, the permeability inferred from this slope, plotted as (0.002, 50,000) in Figure 7, is consistent with the other experiments showing Knudsen transport. We believe that at short times, transport is by liquid flow. In this region, characterized by the line with larger slope in Figure 9, the pore must be filled

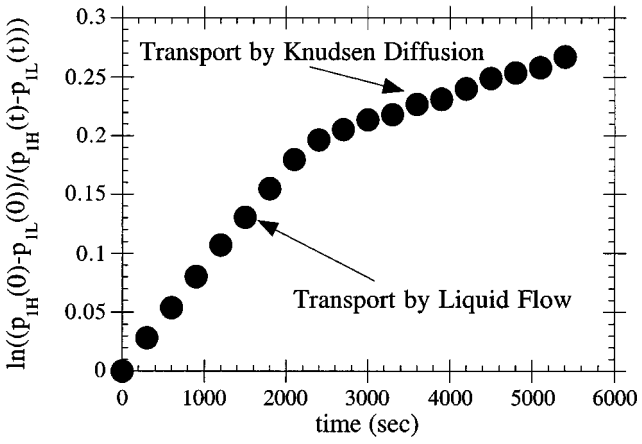

Figure 9. Data for nitrogen at 77 K in a 0.01-μm PCTE membrane plotted according to Eq. 17.

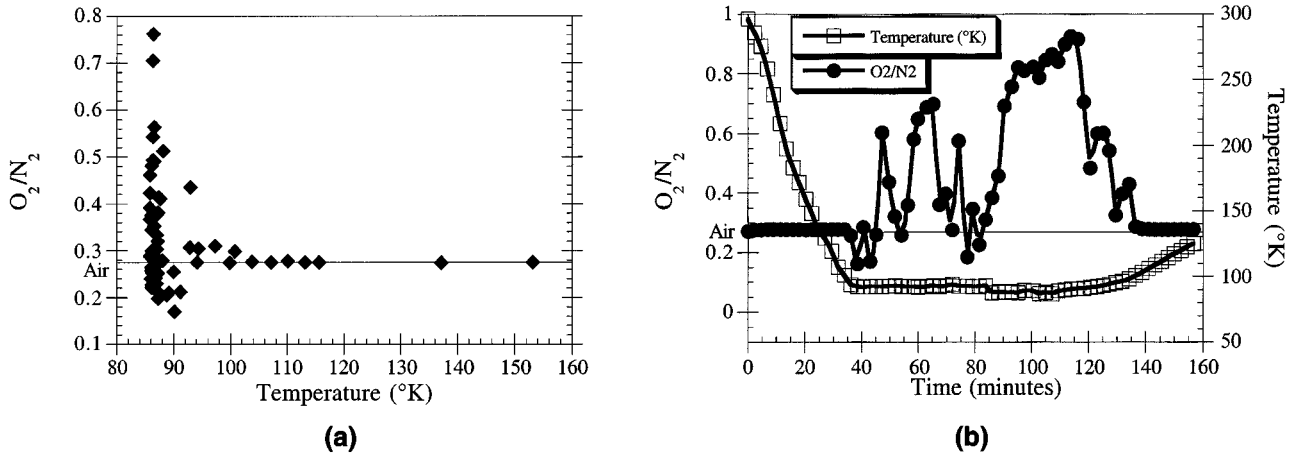

Figure 10. Cryogenic air flow results for the BSCCO superconducting membrane.

with liquid nitrogen since the pressure in the high-pressure compartment exceeds the saturation vapor pressure in the pore. The slope of the data at short times is larger than that predicted for with Poiseuille flow of liquid nitrogen, so it seems to be driven by surface tension.

Finally, we want to explore why earlier experiments with superconducting membranes seemed to separate air. To do so, we abandon the batch experiments fed with oxygen, nitrogen, or helium, basic to the previous results. We switch to flow experiments, detailed in the experimental section of this article, which are continuously fed with air on the high-pressure side. The concentration on the low-pressure side is measured vs. time to determine if any separation occurs.

We made cryogenic flow experiments with porous superconducting and nonsuperconducting membranes. For the superconducting membranes, we obtained data like those of earlier workers, as shown in Figure 10a. This figure shows the effect of temperature on the molar concentration ratio (O_2/N_2) of the permeate. At higher temperatures, this ratio is just 0.27, the ratio in air. At lower temperatures, the ratio varies wildly. It can be 0.2, suggesting a membrane more permeable to nitrogen than to oxygen. It can jump as high as 0.7, suggesting a membrane more permeable to oxygen than to nitrogen. The meaning of these results is somewhat clearer from the plot of permeate concentration and temperature vs. time, shown in Figure 10b. Again, the permeate concentration ratio has the expected value of air at higher temperatures, but begins to oscillate wildly at lower temperatures where superconductivity exists in the BSCCO membrane. Again, the results appear to suggest that superconductivity affects transport, which is inconsistent with our batch diaphragm cell results discussed earlier and summarized in Figure 7.

However, the results for nonsuperconducting membranes in Figure 11 show that the effects in Figure 10 have nothing to do with superconductivity. These data were obtained for cryogenic air flow across a 0.1 μm PCTE membrane, which is certainly not superconducting. Above 100 K, the permeate concentration ratio is equivalent to that of air, 0.27, as shown in Figure 11a. The ratio varies between 0.16 and 0.95 at lower temperatures. As with the superconducting membrane results, the deviation occurs at temperatures greater than the dew point. More specifically, when the permeate concentration and temperature are plotted vs. time, as shown in Figure

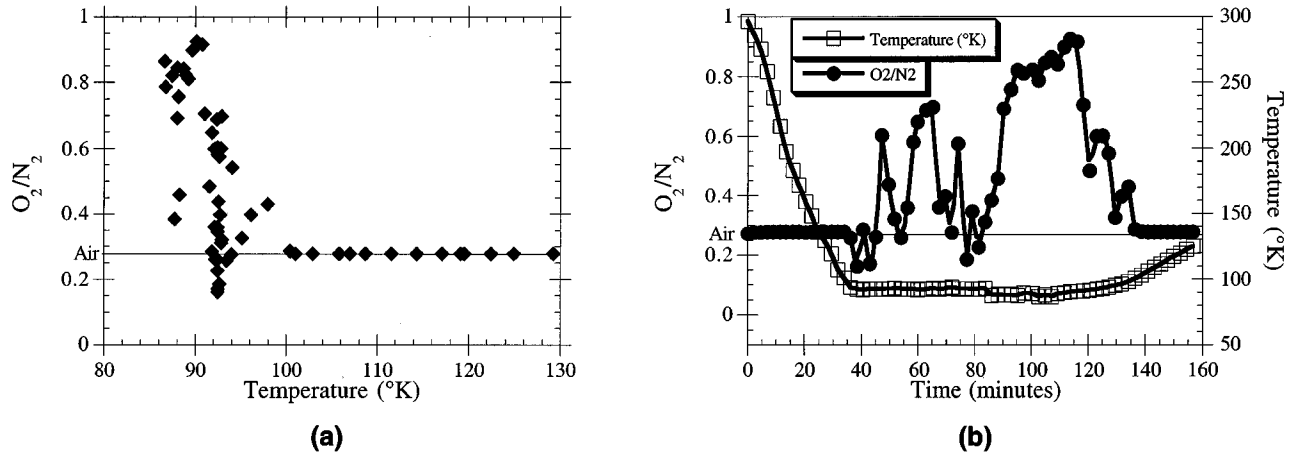

Figure 11. Cryogenic air flow results for the 0.1-μm PCTE membrane.

11b, we see that the concentration ratio begins to oscillate around 98 K, and can be forced to jump still higher by suddenly dropping the temperature from 92 to 87 K.

The conclusion which we draw from Figures 10 and 11 is that these effects have nothing to do with superconductivity. They are almost certainly the results of capillary condensation. At the air pressure used, about 100 torr, vapor will condense in wettable pores at about 84 K. This condensate will be enriched in oxygen. If any pores less than about 0.1 μm in diameter existed in the membranes, then the dew temperature in these pores would have been higher, reflecting a lower saturation pressure as estimated from the Kelvin equation.

If the unexpected effects in this flow experiment are the result of capillary condensation, then liquid enriched in oxygen fills the smaller pores first, and then the larger ones. During this pore filling, the permeate is enriched in nitrogen, as expected from the vapor-liquid equilibrium. When all the pores are filled, the pressure difference forces out the liquid enriched in oxygen, which quickly evaporates to give a pulse of enriched oxygen in the permeate. The process repeats as the empty pores refill with liquid. As a result, the permeate concentration oscillates as shown.

Discussion

The chief conclusion of the experiments in this article is that the superconducting membranes used here do not affect oxygen and nitrogen fluxes. As as result, these membranes are a poor prospect for separating air. The basis of this conclusion comes largely from the results in Figures 6 and 7. These results show that superconducting membranes have the same properties as other porous, nonsuperconducting membranes. They show equivalent permeabilities to oxygen, nitrogen, and helium, both at ambient temperatures (293 K) and at superconducting temperatures (77 K). Moreover, as shown in Figures 10 and 11, the apparent superconducting membrane separations reported in earlier studies also seem to occur in nonsuperconducting membranes operated at similar temperatures. These apparent separations are almost certainly due to capillary condensation.

Our experimental results are consistent with the theoretical models discussed earlier in this article. For each model, the characteristic distance δ indicates when superconductivity will strongly affect oxygen transport. Equation 10 shows that at 77 K, superconducting forces on oxygen molecules, with a magnetic moment of about 2.6×10^{-23} J/T (Stoner, 1926), are strong only at a distance of 1.1 Å from the superconducting surface. The pores in the superconducting membranes used here and in earlier work are about 5 μm, or 50,000 Å. Any short-range forces acting over a distance of δ might be important if transport occurred by surface diffusion. However, the fluxes of helium, nitrogen, and oxygen in all the membranes studied are consistent, as shown in Figures 6 and 7. If surface diffusion were important, the flux of an adsorbed species—nitrogen, for example—should be larger than that expected from the nonadsorbing helium; however, it is not.

In more general terms, these short-range forces are unlikely to affect oxygen transport since these forces are constrained by the penetration depth of the superconductor. At a distance of a few Ångstroms, the magnetic field from an oxygen molecule will penetrate into the superconductor rather than be repelled from it. The Meissner effect will exist only at distances greater than the penetration depth, which is about 100 nm for the superconductors studied here. Again, theory and experiments are consistent.

Thus, the superconducting membranes used in our experiments appear not to work. Could such membranes ever work?

We can imagine four different situations where superconducting membranes might be more useful for air separations. First, the superconducting effects will become longer range at much lower temperatures, as suggested by Eq. 10. However, at these temperatures, air has not only liquefied, but frozen. Separations at such low temperatures have no practical value.

Secondly, the superconducting effects might be more significant for membranes with smaller pores and larger surface areas. After all, the superconductors used here were operated in the Poiseuille flow region, where interactions between the individual molecules and the pore walls were infrequent. If we used smaller pores, we would be in the Knudsen diffusion region, where molecule-wall interactions are the norm. Also, with a higher membrane area, transport by surface diffusion might become more important. We might make membranes which are useful in this limit by growing single crystals of superconductors and then track-etching pores in these single crystals. We feel this small-pore limit should be checked because air separation is so important. However, we don't think superconducting effects will be found because the forces are so short range and constrained by the superconductor's penetration depth.

Thirdly, superconducting membranes might be effective if they did show surface diffusion. In this regard, we are impressed by the studies of Makarshin et al. (1997), who show oxygen adsorption on superconductors decreasing dramatically with temperature. If this decreased adsorption reduced surface diffusion, then the superconducting membranes could become nitrogen selective. We have tried without success (Gordon and Cussler, 1999) to reproduce Makarshin's results, but we may not have duplicated his procedure, which seems incompletely described (Andreev et al., 1994). Our adsorption results, consistent with the batch diffusion results in Figure 7, may also reflect the lack of magnetic interaction between oxygen and the superconductor, since the distance required for repulsion is much smaller than the penetration depth of the magnet.

Finally, we should mention that while oxygen molecules are not affected by superconductivity except at short distances, oxygen droplets may be. A porous superconductor is predicted to exclude 10 μm droplets. We are unsure how this could be used in a separation process. Thus, our results all imply that the prospects are uncertain for air separations based on superconductivity.

Acknowledgments

This work was partially supported by the National Science Foundation (grants CTS 94-28755 and CTS 96-27361) and the Dept. of Defense (DAA H04-95-1-0094). We appreciate the advice of Dr. E. Dan Dahlberg and Dr. Allen Goldman at the University of Minnesota regarding the physics of magnetism and superconductivity. We thank Dr. Joe Schwartz at Praxair, Inc. for obtaining superconducting materials. Ann Gronda took the scanning electron micrographs.

Literature Cited

Andreev, D. V., L. L. Makarshin, and V. N. Parmon, ''Adsorption of Oxygen and Nitrogen Molecules on a Superconducting Adsorbent (in Russian),'' *Supercond. Phys. Chem. Technol.*, **7**, 884 (1994).

Bourdillon, A., and N. X. Tan Bourdillon, *High Temperature Superconductors: Processing and Science*, Academic Press, Boston, p. 206 (1994).

Brunauer, S., *The Adsorption of Gases and Vapors*, Princeton University Press, Princeton, p. 120 (1945).

Carman, P. C., *Flow of Gases Through Porous Media*, Academic Press, New York, p. 125 (1956).

Cussler, E. L., *Diffusion: Mass Transfer in Fluid Systems*, second ed., Cambridge University Press, Cambridge, p. 22 (1997).

Dodge, B. F., and A. K. Dunbar, ''An Investigation of the Coexisting Liquid and Vapor Phases of Solutions of Oxygen and Nitrogen,'' *J. Amer. Chem. Soc.*, **3**, 591 (1927).

Gordon, R. D., ''Transport of Condensable Gases Through Porous Media,'' PhD Thesis, Univ. of Minnesota, Minneapolis (1998).

Gordon, R. D., and E. L. Cussler, ''Adsorption of Oxygen on $YBa_2Cu_3O_{7-x}$ and $(Bi,Pb)_2Sr_2Ca_2Cu_3O_x$ Superconducting Adsorbents,'' *Langmuir*, **15**, 3950 (1999).

Gregg, S. J., and K. S. W. Sing, *Adsorption, Surface Area, and Porosity*, Academic Press, London, p. 116 (1982).

Hellman, F., E. M. Gyorgy, D. W. Johnson, Jr., H. M. O'Bryan, and R. C. Sherwood, ''Levitation of a Magnet Over a Flat Type II Superconductor,'' *J. Appl. Phys.*, **63**, 447 (1988).

Jackson, J. D., *Classical Electrodynamics*, Wiley, New York, p. 156 (1962).

Koros, W. J., and G. K. Fleming, ''Membrane-Based Gas Separation,'' *J. Memb. Sci.*, **83**, 1 (1993).

Lee, K. H., and S. T. Hwang, ''The Transport of Condensible Vapors Through a Microporous Vycor Glass Membrane,'' *J. Coll. Interf. Sci.*, **110**, 544 (1986).

Louie, B., ''Permeation of Fluid Through Ceramic Materials,'' PhD Thesis, Oxford Univ., Oxford, U. K. (1993).

Makarshin, L. L., D. V. Andreev, and V. N. Parmon, '''Levitation' of Paramagnetic Oxygen Molecules Over the Surface of High Temperature Superconductor,'' *Chem. Phys. Lett.*, **266**, 173 (1997).

Mason, E. A., and B. Kronstadt, ''Graham's Laws of Diffusion and Effusion,'' *J. Chem. Educ.*, **44**, 740 (1967).

Mason, E. A., and R. B. Evans, III, ''Graham's Laws: Simple Demonstrations of Gases in Motion,'' *J. Chem. Educ.*, **46**, 358 (1969).

Mason, E. A., and A. P. Malinauskas, *Gas Transport in Porous Media: The Dusty Gas Model*, Elsevier, Amsterdam (1983).

Meixner, D. L., and P. N. Dyer, ''Characterization of the Transport Properties of Microporous Inorganic Membranes,'' *J. Memb. Sci.*, **140**, 81 (1998).

O'Neil, M. E., and F. Chorlton, *Viscous and Compressible Fluid Dynamics*, Ellis Horwood Ltd., Chichester, U. K., p. 269 (1989).

Orlando, T. P., and K. A. Delin, *Foundations of Applied Superconductivity*, Addison-Wesley, Reading, p. 577 (1991).

Prasad, R., F. Notaro, and D. R. Thompson, ''Evolution of Membranes in Commercial Air Separation,'' *J. Memb. Sci.*, **94**, 225 (1994).

Robeson, L. M., ''Correlation of Separation Factor vs. Permeability for Polymeric Membranes,'' *J. Memb. Sci.*, **62**, 165 (1991).

Reich, S., and I. Cabasso, ''Separation of Paramagnetic and Diamagnetic Molecules Using High-T_c Superconducting Ceramics,'' *Nature*, **388**, 330 (1989).

Rose-Innes, A. C., and E. H. Rhoderick, *Introduction to Superconductivity*, Pergamon Press, Oxford (1969).

Ross, S., and J. P. Olivier, *On Physical Adsorption*, Wiley-Interscience, New York, p. 31 (1964).

Sawai, Y., N. Bamba, K. Ishizaki, and S. Hayashi, ''A Superconducting Filter to Separate Oxygen and Argon Mixture,'' *J. Porous Mater.*, **2**, 151 (1995).

Sircar, S., and M. B. Rao, ''Estimation of Surface Diffusion Through Porous Media,'' *AIChE J.*, **36**, 1249 (1990).

Stoner, E. C., *Magnetism and Atomic Structure*, E. P. Dutton and Co., New York, p. 126, 142 (1926).

Uhlhorn, R. J. R., K. Keizer, and A. J. Burggraaf, ''Gas Transport and Separation with Ceramic Membranes. Part I. Multilayer Diffusion and Capillary Condensation,'' *J. Memb. Sci.*, **66**, 259 (1992).

Yang, R. T., *Gas Separation by Adsorption Processes*, Butterworths, Boston (1987).

Manuscript received Sept. 15, 1998, and revision received Aug. 3, 1999.